MARTIN MARIETTA ENERGY SYSTEMS LIBRARIES

3 4456 0287020 3

ORNL/TM-11937

OAK RIDGE NATIONAL LABORATORY

MARTIN MARIETTA

Preliminary Engineering Studies for the Support Shell of the Outer Tracker of the SDC Detector

David H. Vandergriff

OAK RIDGE NATIONAL LABORATORY
CENTRAL RESEARCH LIBRARY
CIRCULATION SECTION
4500N ROOM 175
LIBRARY LOAN COPY
DO NOT TRANSFER TO ANOTHER PERSON
If you wish someone else to see this report, send in name with report and the library will arrange a loan.

September 1991

MANAGED BY
MARTIN MARIETTA ENERGY SYSTEMS, INC.
FOR THE UNITED STATES
DEPARTMENT OF ENERGY

This report has been reproduced directly from the best available copy.

Available to DOE and DOE contractors from the Office of Scientific and Technical Information, P.O. Box 62, Oak Ridge, TN 37831, prices available from (615) 576-8401, FTS 626-8401.

Available to the public from the National Technical Information Service, U.S. Department of Commerce, 5285 Port Royal Rd., Springfield, VA 22161.

This report was prepared as an account of work sponsored by an agency of the United States Government. Neither the United States Government nor any agency thereof, nor any of their employees, makes any warranty, express or implied, or assumes any legal liability or responsibility for the accuracy, completeness, or usefulness of any information, apparatus, product, or process disclosed, or represents that its use would not infringe privately owned rights. Reference herein to any specific commercial product, process, or service by trade name, trademark, manufacturer, or otherwise, does not necessarily constitute or imply its endorsement, recommendation, or favoring by the United States Government or any agency thereof. The views and opinions of authors expressed herein do not necessarily state or reflect those of the United States Government or any agency thereof.

ORNL/TM-11937

Preliminary Engineering Studies for the Support Shell of the Outer Tracker of the SDC Detector

David H. Vandergriff
Engineering Division

September 1991

Contributing Author:

John Mayhall

Prepared by the
OAK RIDGE NATIONAL LABORATORY
Oak Ridge, Tennessee 37831
managed by
MARTIN MARIETTA ENERGY SYSTEMS, INC.
for the
U.S. DEPARTMENT OF ENERGY
under Contract No. DE-AC05-84OR21400

MARTIN MARIETTA ENERGY SYSTEMS LIBRARIES

3 4456 0287020 3

Table of Contents

Page

Figures IV

Table IV

Abstract V

1.0 Introduction 1

2.0 Support Shell Requirements 1

3.0 Cylindrical Shell Evaluation 2

3.1 Shell Physical Analysis 2

3.2 Shell Cost Analysis 4

4.0 Modular shell Evaluation 8

4.1 Shell Physical Analysis 8

4.1.1 Buckling of Sides of Trough 10

4.1.2 Buckling of Lid Top 12

4.1.3 Bugling Due to Straw Pressure 13

5.0 Conclusion 20

FIGURES

Figure		Page
1	Cylindrical Support Shell Tracking Element Arrangement	1
2	Modular Support Shell Tracking Element Arrangement	2
3	Structural Tube Typical Dimensions	3
4	NASTRAN Analysis Results	5
5	MSC/CAASE Analysis Results	5
6	Material Layup of Trough Sides	11
7	Module Lid Top	12
8	Straw Tracking Element Forces and Material Layup	13
9	Straw Tracking Element Segment	14
10	Lid Top Dimensions	17

TABLE

Table		
1	First Unit Cylinder Fabrication Cost Estimate	7

Abstract

The Solenoidal Detector Collaboration (SDC) detector is in the conceptual design phase. ORNL is currently working with various sub-groups on the design of the outer tracker portion of the SDC detector. A major focus in the outer tracker design is the structure that mounts and supports the tracking elements. This structure must meet extreme requirements of alignment and stability while containing a minimum of material. This report describes the requirements, evaluations, and analyses that have been performed on the two options being explored; a cylindrical support shell and a modular support shell.

Preliminary Engineering Studies
for the Support Shell of the
Outer Tracker of the SDC Detector

1.0 Introduction

The outer tracker of the Solenoidal Detector Collaboration (SDC) is in the initial phase of engineering design. Mechanical engineering of the outer tracker consists of mounting and supporting the straw tube (wire) and/or plastic scintillating fiber (PSF) tracking elements. The support and mount must provide an extremely stable platform onto which detector tracking elements are mounted. This platform must meet the requirements of precision alignment and location for the tracking elements. Various configurations of these elements have been proposed for use within the tracker design envelope. Preliminary studies of potential mounting schemes for these tracking elements have revealed two support shell options; the cylindrical support shell and the modular support shell. Engineering and physics studies of the outer tracker have provided the basis for the selection of the two options described in this report.

2.0 Support Shell Requirements

The support shell for the SDC outer tracker must provide a lightweight, low radiation length structure that is radiation hardened and is stable under thermal variations. Analysis has revealed that the location of the tracking elements must be known to 30 microns, 400 microns and 300 microns for circumferential, radial and longitudinal location, respectively. Two methods for achieving these goals are discussed here. The first method utilizes a precision cylinder with tracking elements placed directly on the cylinder's surface (Figure 1). Small modular support shells are used in the second method (Figure 2). Tracking elements are placed in the precision modular shells, which are then placed onto a less precise cylindrical support shell. Tolerances are met by placing the modules on precision machined rings which encircle the cylindrical support shell. Both methods are being evaluated to determine the feasibility of the designs.

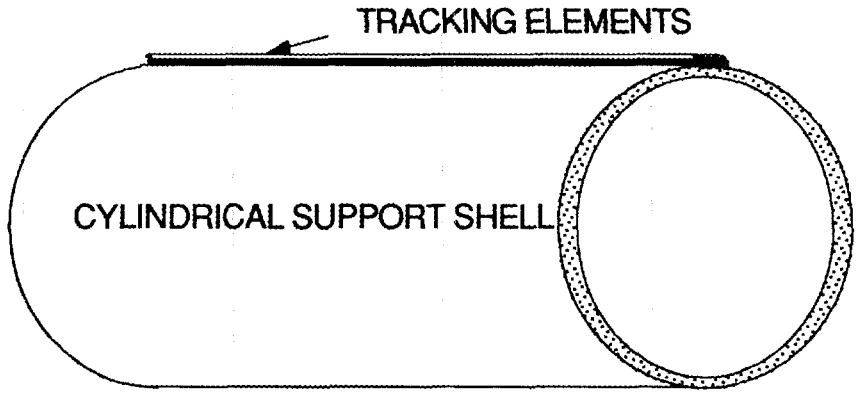

FIGURE 1 - Cylindrical Support Shell Tracking Element Arrangement

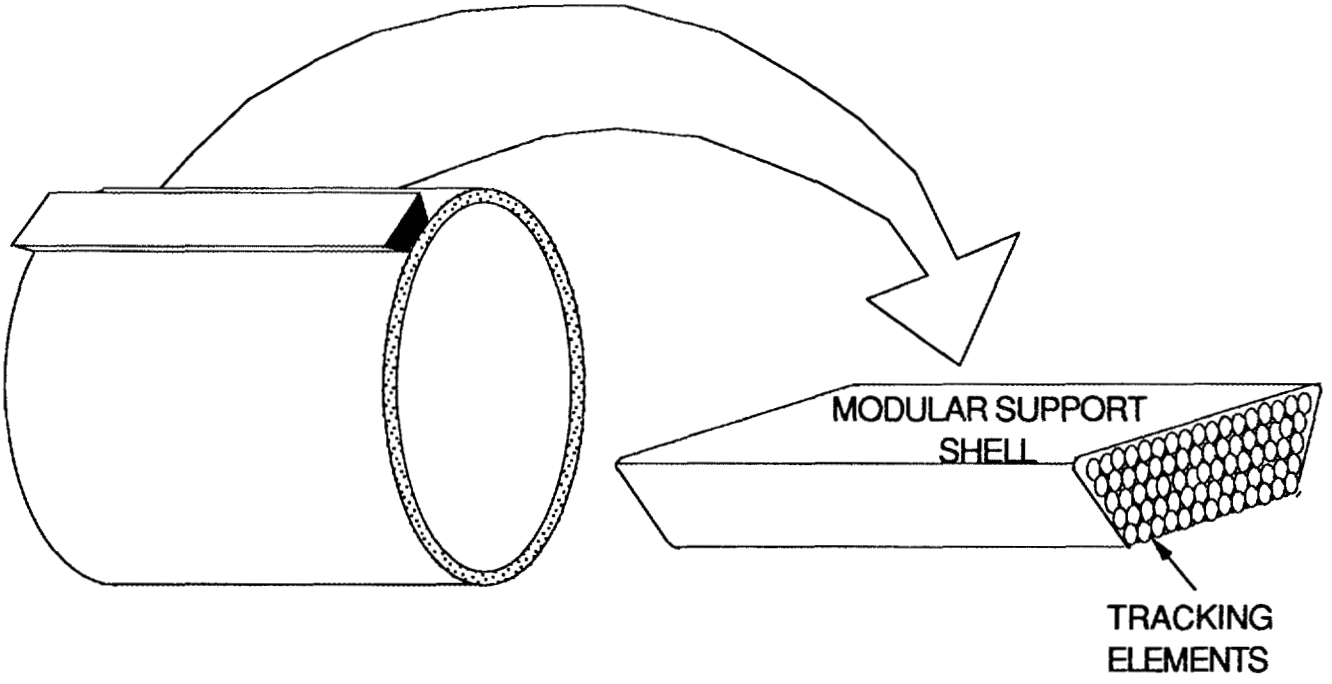

FIGURE 2 - Modular Support Shell Tracking Element Arrangement

3.0 Cylindrical Shell Evaluation

The outer tracker for the SDC detector requires a stable structure to mount the straw and fiber elements on. The use of a cylindrical shell fabricated from carbon composite based materials will provide this stable base. Analysis has been performed on both the physical properties of this structure and the cost for fabrication. The following sections detail the progress made in both endeavors.

3.1 Shell Physical Analysis

The cylindrical shell must provide a lightweight, low radiation length structure that is radiation hardened, and provides superior thermal stability. The cylinder must achieve the alignment requirements dictated by the physics. The alignment of each superlayer is simplified when each element can be registered from a common surface. This registration requires maximum stability under load. In addition to the requirements of the physics involved, the base structure must be simple to fabricate and assemble. The structural integrity of the cylindrical shell has been evaluated.

Cylinders used for the support of the tracking elements must exhibit minimum bending and deflection, and resist compression loading. Additionally, the cylinder design must prevent sag or local distortions. The ends of the cylindrical shell must have sufficient hoop strength to support the end plates, and finally, the carbon fibers used to make up the tube must be stable under varying environmental and physical loading conditions.

The cylinder size chosen for assessment is based on the outer tracker description in the SDC Expression of Interest (EOI) document. An 80 cm radius cylinder, 6 meters long (Figure 3) is used. This cylinder is representative of the inner superlayer in the outer tracking volume of the Central Tracking Chamber (CTC). It is also the smallest cross section cylinder and therefore provides the most conservative results for the bending analysis. An initial cylinder thickness of 2.54 cm was chosen, based on the results of the standard beam deflection calculation shown below.

$$\text{Deflection} = \frac{5WL^4}{384EI}$$

where:

$W = .59$ KG/CM
$L = 600$ CM
$E = .703 \times 10^6$ KG/CM^2
$I = 2297116$ CM^4

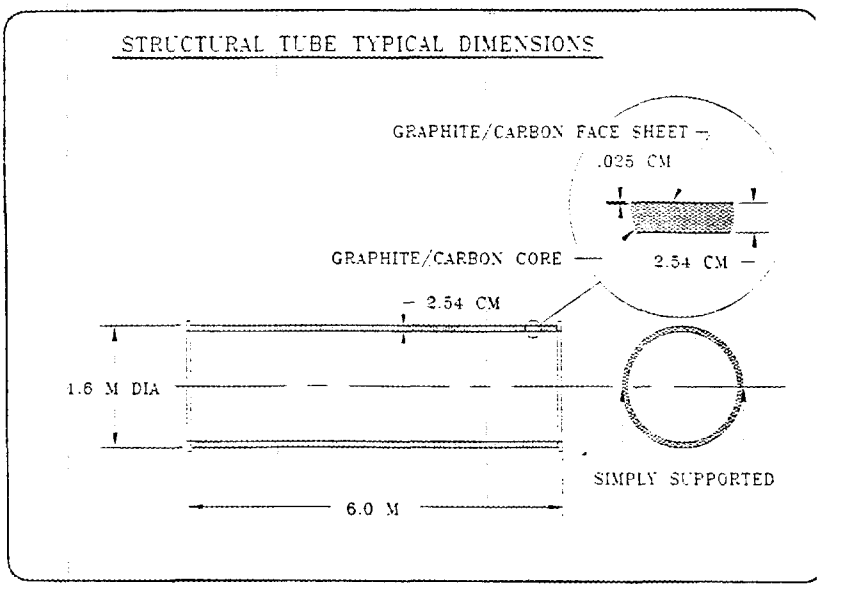

FIGURE 3 - Sructural Tube Typical Dimensions

This analysis assumes that the tube is simply supported, that the tube retains its circular cross section throughout its entire length, and that the 2.54 cm thickness is solid and has the modulus of elasticity of 10,000,000 psi, a typical value for carbon-based materials. Based on these assumptions, the deflection was found to be less than 50 microns. This preliminary cylinder evaluation provides a basis for the in-depth finite element analyses that followed.

A series of finite element analyses (FEA) were done on the cylinder using models of increasingly more accurate and refined values for material properties and layup across the 2.54 cm thickness. The first FEA run duplicated the conditions described above, providing comparable results. This verified both the FEA model geometry as well as the hand calculations. Subsequent calculations lead to the final analysis presented here, based on the superlayer cross section described above.

The second FEA runs were performed on a cylinder with a "face sheet-core-face sheet" shell construction. This type of construction provides high bending stiffness with much lower mass than a solid cylinder. For analysis purposes, the material tensile modulus of the two carbon face sheets was set at $.7 \times 10^6$ KG/CM^2. This value was determined using the GENRAD composite material analyzer code. The program allows the user to input varying composite materials and layup orientations and receive material structural properties as output.

Standard strength IM6 composite material was chosen for the analysis. A wind pattern of 90/0/90 was used to give a symmetric layup with the properties of a quasi-isotropic material, i.e., the same material properties in both the axial and transverse directions. This layup provides a structure that is structurally stable and resistant to distortions in thermal cycling conditions.

A carbon honeycomb core was used, based on the properties of the Hexcel Corporation HFT-G-3/16-6.0 Graphite Reinforced Honeycomb core. Any similar core material may be chosen because the analysis code, MSC/NASTRAN, ignores the bending properties of core material and only requires input of the shear modulus. The shear modulus included in this analysis is sufficiently low that it does not affect the results of the bending analysis and is representative of any number of core materials, including foam. Core material properties primarily affect the shear deflection of the structure.

The FEA performed on the cylindrical shell was used to calculate the bending and sag properties only. Figure 4 displays the results of this analysis as performed on Nastran and post-processed using the PATRAN program. The FEA was verified using NASTRAN, NISA, and a PC-based analysis tool, MSC/CAASE (Figure 5). An additional check was made using a baseline analysis of a face sheet-core-face sheet structure. The results of each method agreed, providing a high degree of confidence in the results obtained.

Based on the accumulated results of these analyses, the basic cylinder is sufficiently stable to be used with confidence as a support structure for the straw tube and scintillating fiber tracking elements. The low deflection and radiation length of the structure meet the design requirements for the outer tracker. Additional analyses will be performed to optimize the material sizing and further reduce the radiation lengths.

3.2 Shell Cost Analysis

Recent evaluation of the cylinders used to support the tracking components of the outer tracker has centered around fabrication methods, and the cost associated with cylinder production. The basic assumptions for the stable base cylinder are: full length continuous cylinders; .015" to .020" wall thickness; graphite fiber reinforced epoxy composite; integral end rings with, possibly, intermediate stiffeners; and cylinder support from the ends only. An attempt has been made to produce an accurate cost analysis of the cylinders using these criteria and the dimensions provided for the "baseline" tracker design.

Many cost drivers will affect the estimate for fabrication of the required cylinders. The two principle drivers are cylinder size and required precision. Secondary variables are important, however, because performance requirements could elevate any of them to major importance. A few comments about the secondary variables are in order before discussing the cost estimate in terms of size and precision.

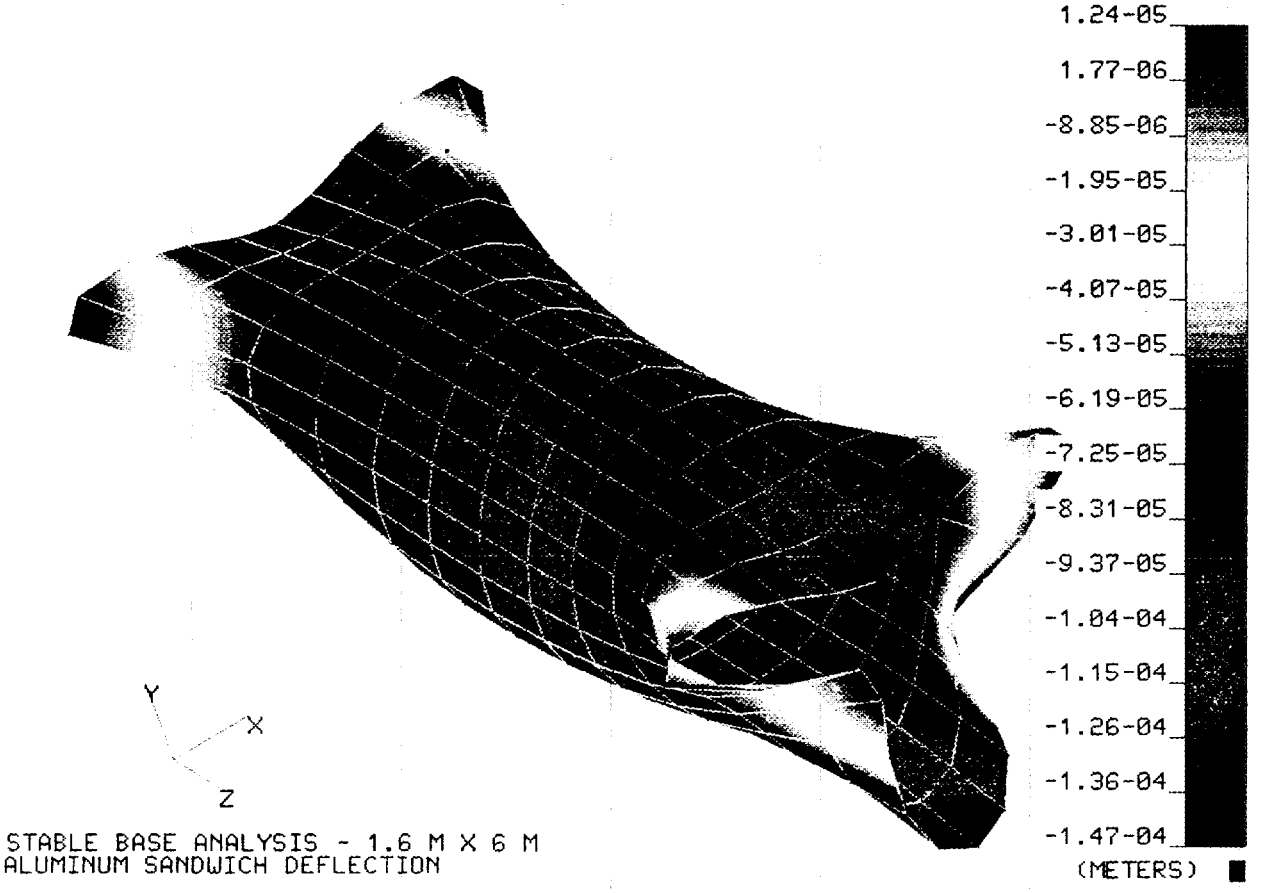

FIGURE 4 - NASTRAN Analysis Results

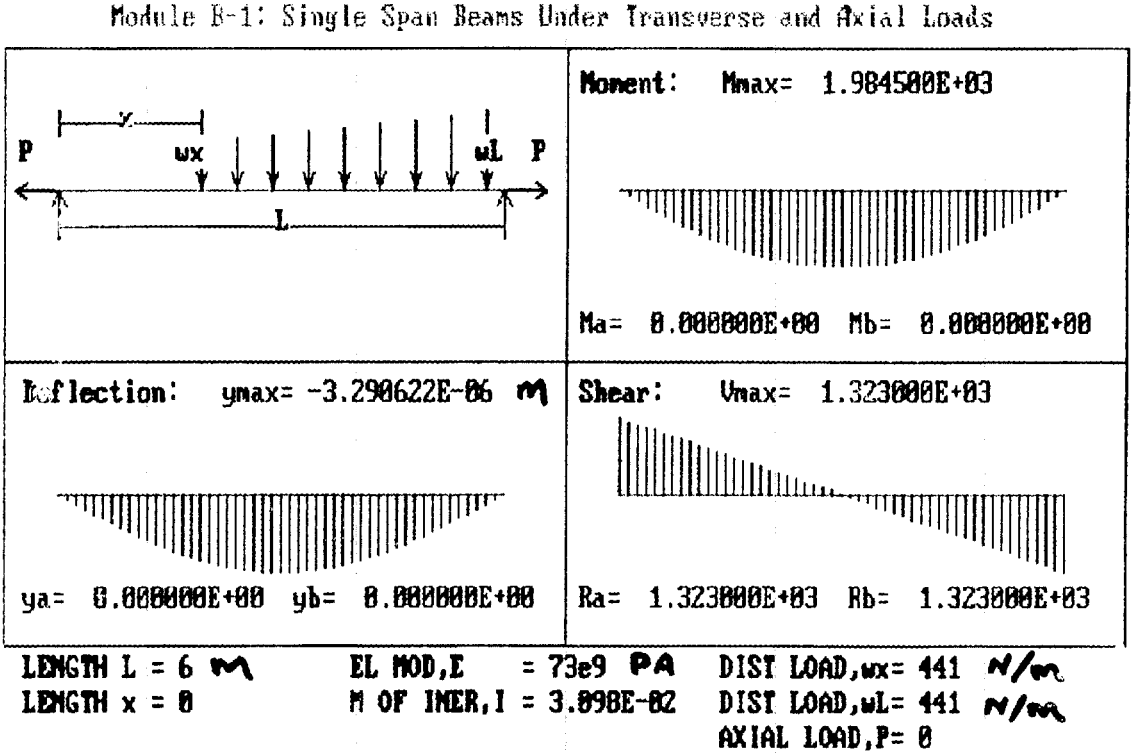

FIGURE 5 - MSC/CAASE Analysis Results

The graphite fiber reinforced epoxy composite material has been chosen because it has a high specific strength and stiffness, low weight, and the material is expected to have a small influence on the performance of the detector. There are unknowns associated with this material: dimensional stability as a result of temperature changes or viscoelastic creep, and long term effects of the operational radiation environment.

Within the graphite/epoxy composite itself, the assumption is that the fiber modulus requirement will be less than 55 msi. This assumption is based on preliminary analysis of the strength requirements of the cylinder. Higher modulus fibers are readily available, but these tend to have very low strength and are difficult to use in high precision fabrication environments. Fibers which are both high in strength and modulus are available for special applications, and will be used if required.

The cylinder wall construction is assumed to be a wet wound, three layer 90/0/90 wall of .005" material providing a total thickness of .015". Additional evaluation and analysis must be performed to determine if this construction will meet mechanical design requirements. If thickness must be increased or the construction method modified, the effect of the presence of the cylinder on detector performance will become increasingly important. The relative effect of another construction method on the cost will be measurable but not a significant driver at this time.

A cost estimate for the first cylinder is presented in terms of cylinder O.D. and required precision (cylindricity) in Table 1. The estimates include the cost of a fabrication mandrel, winding attachments, and cylinder production tooling. Estimates do not include generic tooling such as the winding machine, cranes or other necessary handling equipment. The finished cylinder length has been set at 5 meters for this cost analysis. Mandrels are assumed to be chrome plated steel. The estimate is based upon informal discussion with mandrel suppliers, winding technology facilities, and potential fabricators. Previous experience at ORNL also was used in the estimates.

The cost estimates are also driven by some hidden considerations. The state of the art in this technology is not advanced sufficiently to build all possibilities without incurring R & D charges. These additional costs are contained in the estimates for the large diameter, high precision cylinders (the lower left quadrant of the table). Conversely, the smaller, less precise cylinders in the upper right quadrant can be produced by several manufacturers without difficulty. Between these regions, there is an increasing amount of sophistication and capability required. For the baseline design, the smaller cylinders will be used for the fiber technology, which requires greater precision for mounting. The larger cylinders will be used for straw tracking which does not require the degree of precision necessary for the fibers. The fiber cylinders would have cylindricity requirements in the .005" range, and the straw cylinders in the .010" range.

Further evaluation is required to determine the final structural requirements of the cylinder. These requirements will feed directly into the cost estimate and physics performance capabilities of the tracker. These evaluations will continue in concert with the continued refinement of the straw tube and fiber tracking technologies, which will be mounted to the cylinders.

TABLE 1- First Unit Cylinder Cost Estimate Including Fabrication Mandrels

TOTAL COST ($K)

CYLINDRICITY REQUIREMENT (IN.)

CYL. O.D. (FT)	0.001	0.002	0.005	0.010	0.020
4.4	660	330	182	173	145
5.2	1870	390	315	205	170
6.6	2375	1190	400	258	216
7.8	2810	1405	585	450	255
9.2	3310	1655	1380	635	442
10.5	3780	1890	1575	722	590

4.0 Modular Shell Evaluation

The modular shell design for the outer tracker of the SDC provides a method for holding the straw tracking elements in position and maintaining their alignment along the length of the module. The modules will be constructed of carbon-based composites and will span a length equal to half the overall outer tracker length. They will be supported along this length at approximately 80 cm intervals. The modules will be attached to a cylindrical shell similar to the one described above, which will provide the overall structural integrity of the system. The modular design provides for testing of individual units prior to assembly into an overall tracking unit. This report contains the results of the physical analysis of the shell as well as specifications for the fabrication of a prototypical modular shell.

4.1 Shell Physical Analysis

The modular shell is designed to the same basic requirements as the cylindrical shell. This includes bending loads, compression loads and thermal loads. Additionally, due to the small size of the modular shell, thermal stresses are incurred in the manufacture of the shell that require special provisions to prevent distortion of the shell. The nature of these loads, the stresses that they produce, and the material layup required to negate them have been evaluated.

The thermal loads that result when a modular shell is cured and then returned to room temperature determine the design of the modular shell. The stress-free temperature of a cured composite is close to the maximum cure temperature at which most of the cross-linking occurs in the polymer used for the matrix. Due to the high coefficient of thermal expansion (CTE) of the epoxy and the negative CTE of the graphite, compressive buckling stress are induced in the graphite filament.

The induced compressive stresses in the thin laminates due to cooling from cure result in various modes of buckling, causing warping and waviness of the modules. To resolve this problem, a design consisting of a face sheet-core-face sheet layup was contrived. This design, using a foam core, saves weight over that of the solid laminate for the case of designing to prevent buckling due to compressive loads. This layup requires three layers of .0015 inch graphite on each side of the foam core. This layup, as in the case of the cylindrical shell, provides a balanced and symmetric structure capable of resisting physical loads and fabrication loads.

There are two types of residual stresses, shearing residual stresses between plies and between epoxy matrix and graphite filament. The residual stresses between plies are due to each ply of the laminate being differently oriented (e.g., ±30° layup), which causes each ply to have different coefficients of thermal expansion in different directions. These differences induce shearing forces between plies and cause warpage if the layup is not balanced and symmetric about the centroidal center line of the layup. If balanced and symmetric, however, the forces sum to zero and generally cause no trouble. Additionally, these stresses can be determined using finite-element laminated analysis, using the maximum curing temperature as zero stress

temperature, and cooling back to room temperature, and reading out the resulting residual stresses.

The residual stresses between epoxy matrix and graphite filament are due to the enormous differences between graphite filament COE (coefficient of thermal expansion) and the epoxy COE. Again, these stresses do not cause warpage, providing the layup is symmetric and balanced about the centroidal plane. These stresses cannot be determined by laminated finite-element analysis. One would need to perform a "micro-finite-element" analysis, modeling individual elements of epoxy and elements of graphite in order to determine these stresses. These stresses can cause buckling of thin elements because of the net compressive forces which they produce in the graphite filaments. The following example can aid in this understanding. The current layup is as follows:

[0/+30/-30/-30/+30/0] .0025" per ply. The properties of this layup have been determined by finite element analysis to be:

$$E_0 = 20.0(10)^6 \text{ psi}$$
$$E_{90} = 2.14(10)^6 \text{ psi}$$
$$G = 5.29(10)^6 \text{ psi}$$
$$\text{COE} = \alpha$$
$$\alpha_0 = \frac{-1.382(10)^6}{°F}$$
$$\alpha_{90} = \frac{6.315(10)^{-6}}{°F}$$

If the layout is treated as two bars for an approximate analysis, one bar is graphite with a COE of α_0 and the other will be epoxy with a COE of

$$\frac{21.0(10)^{-6}}{°F}, \alpha_e.$$

The equation that expresses the behavior of the two bars during cooling is as follows:

$$\Delta T(\alpha_e - \alpha_o) = \frac{P}{A_g E_g} + \frac{P}{A_e E_e}$$

Equation 1

Where

ΔT = Cure Temperature – Room Temperature

P = induced compressive force in graphite, equal to tensile force in epoxy

A_g = cross sectional area of graphite

A_e = cross sectional area of epoxy

(A_g =.60 ; A_e =.40)

E_g = Modulus of graphite = $E_o = 20(10)^6$

E_e = Modulus of epoxy = $1.0(10)^6$ psi

However, the shear behavior will induce a force of P (Equation 1). To determine the compressive stresses in the graphite, using Equation 1:

$$10^{-6}(350-70)[21.0-(-1.382)] = P\left[\frac{1}{.4(10)^6} + \frac{1}{.6(20)10^6}\right]$$

or $P = 2426$ lb

$$\text{Compressive Stress in Graphite} = \frac{P}{A_g} = \frac{-2426}{.6}$$

$$= -4043 \text{ psi}$$

The equation

$$\frac{P}{A_g} \approx \Delta T \quad 14.0$$

will give a good estimate of the compressive stresses (that tend to buckle) induced in the curing ΔT. Obviously, we would like ΔT to be as low as possible.
Such residual compressive stresses would be no problem in thick laminates or in supported thin laminates; i.e., thin face sheets bonded to honeycomb or foam sandwich.

Thus, buckling or crippling can occur during cure.

4.1.1 Buckling of Sides of Trough

From Timoshenko's Theory of Elastic Stability, 1st Edition, 1936, page 339,

$$\sigma_{cr} = \frac{K\pi^2 D}{b^2 h} \qquad \text{Equation 2}$$

Where

$$K = .456 + \left(\frac{b}{a}\right)^2 = .456 + \left(\frac{1.403}{39.37}\right)^2 = .457$$

$$D = I\sqrt{(E_0 E_{90})}$$

I = Bending moment of Inertia of cross section per running inch.

For our 6-ply $[0/30/-30]_S$, layup,

h = .015 in ; thickness
a = 39.37 in; length
b = 1.403 in; width

$$I = \frac{(.015)^3}{12} = 2.81(10)^{-7}\frac{in^4}{in}$$

and E_0 and E_{90} are the flexural moduli in the 0° direction [$20(10)^6$ psi] and 90° direction [$2.14(10)^6$ psi], respectively.

Thus from Equation 2:

$$\sigma_{cr} = \frac{.457\pi^2\sqrt{20(2.14)}\,10^6(2.81)10^{-7}}{(1.403)^2(.015)} = 281 \quad psi$$

Since the residual compressive stress is 4043 psi, the side will buckle. An alternative design is:

$$I = (.005)\left(\frac{h'}{2}\right)^2 2 + \frac{(.005)^3}{6} = .0025h'^2 + 2.08(10)^{-7} = .0025\left[h'^2 + 8.33(10)^{-6}\right]$$

$$E_0 = 19.8(10)^6 \text{ psi}$$

$$E_{90} = 3.5(10)^6$$

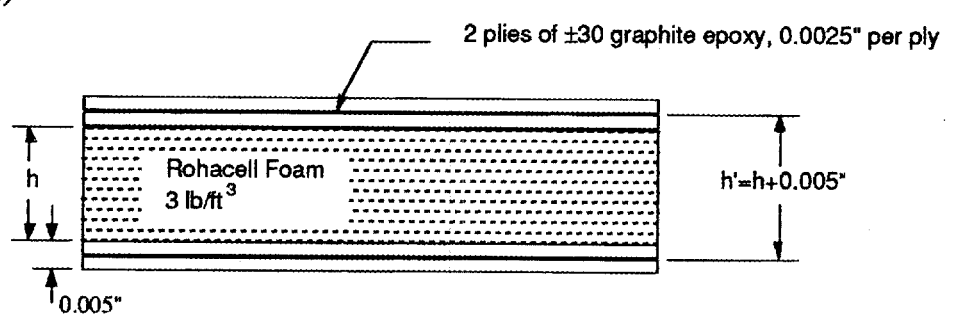

FIGURE 6 - Material Layup of Trough Sides

Solve for h' required to give factor of safety of 2.

$$2(4043) = \frac{.457\pi^2\sqrt{19.8(3.5)}\,10^6(.0025)\left[h'^2 + 8.33(10)^{-6}\right]}{(1.403)^2(.010)}$$

$h' = .0411$

$h = .0411 - .005 = .0361$

Rohacell's thinnest foam is 1 mm, or .0394-in. This material is sufficient.

4.1.2. Buckling of LID TOP

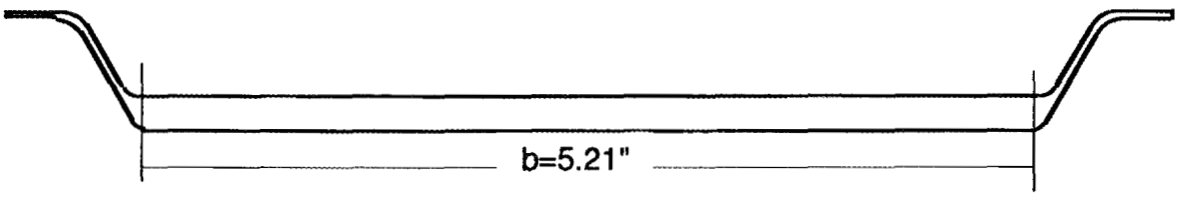

FIGURE 7 - Module Lid Top

Treated as a plate, a inches long, b inches wide, simply supported all around, with axial compressive stresses of 4043 psi (page 10), using Timoshenko reference, page 329, eqn. 213, K = 4.

$$\sigma_{cr} = \frac{(N_x)_{cr}}{h} = \frac{4\pi^2 D}{b^2 h} \qquad \text{Equation 3}$$

or

$$\sigma_{cr} = \frac{4\pi^2\sqrt{E_0 E_{90}}\,h^3}{b^2 h\ 12} = \frac{\pi^2\sqrt{E_0 E_{90}}}{3}\left(\frac{h}{b}\right)^2$$

for the solution described,

$$\sigma_{cr} = \frac{\pi^2}{3}\sqrt{20(2.14)}\,10^6\left(\frac{.015}{5.21}\right)^2 = 178\ \text{psi}$$

With a residual compressive stress of 4043 psi, the plate will buckle. For the design using $I = .0025\left[h'^2 + 8.33(10)^{-6}\right]$ and with the layup [30/-30/foam/-30/30] .0025 in. per ply, at a cure temperature of 200°F, a stress $(\sigma = 14\Delta T)$ of -1820 psi is developed. Determine the foam thickness required to prevent buckling. Equation 2 becomes:

$$2(1820) = \frac{4\pi^2\sqrt{19.8(3.5)}(.0025)\left[h'^2 + 8.33(10)^{-6}\right]10^6}{(5.21)^2(.010)}$$

or $h'^2 + 8.333(10)^{-6} = .0012026$

$h' = .0346$

$h = .0296$

Thus .030-in foam would be required to prevent this buckling.

4.1.3. Bulging Due to Straw Pressure

The module lid top and trough bottom will squeeze the straws together. They will be squeezed down against the wire supports, which are spaced every 80 cm (31.5"). While clamped in this squeeze, the lid will be bonded onto the trough. Because of compliance of the straw, it will exert pressure back against the lid and trough after removal from the bonding fixture, causing bulging, analyzed as follows:

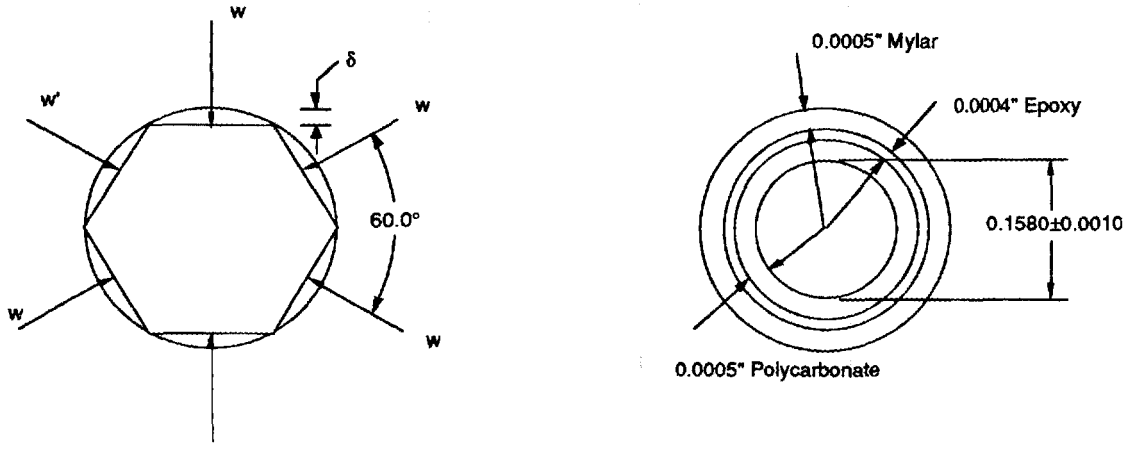

FIGURE 8 - Straw Tracking Element Forces and Material Layup

The force W (applied on 6 sides) can be determined versus deflection, δ from Roark, 5th Edition, page 226, case 7 as follows:

$$\delta = \frac{WR^3}{EI}\left[\frac{1}{4\sin^2\theta}\left(\theta K_1 + \frac{\sin^2\theta}{2}K_3\right) - \frac{1}{2\theta}\right]$$

Equation 4

The properties of the straw materials are as follows:

Material	Mylar	Epoxy	Polycarbonate
Specific Gravity	.920	1.35	1.20
Young's Modulus, psi	25,000	200,000	330,000
Ultimate Strength, psi	1,500	5,000	9,000
Elongation, %	--	--	100
CTE	$\frac{90(10)^{-6}}{°F}$	$\frac{30(10)^{-6}}{°F}$	$\frac{37.5(10)^{-6}}{°F}$

Determine EI of Wall of straw in bending for a 1" section

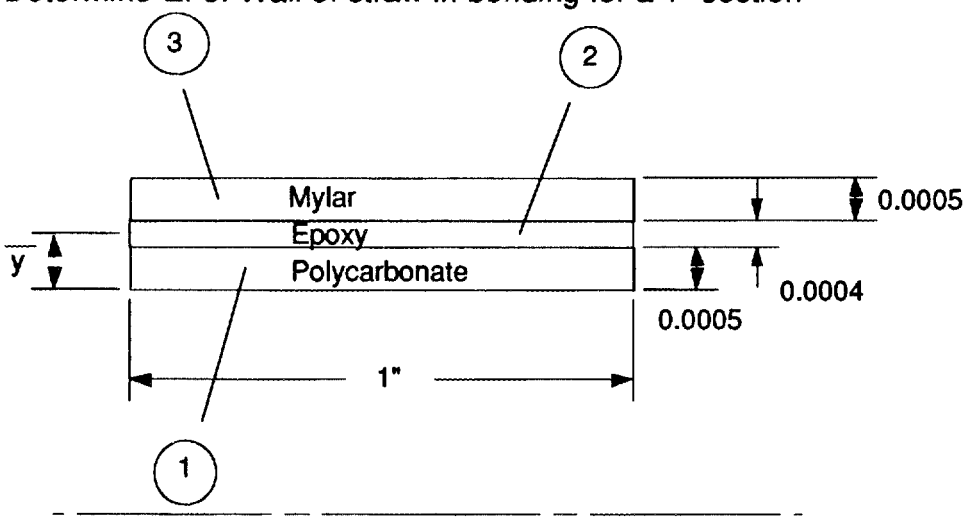

FIGURE 9 - Straw Tracking Element Segment

E	Item	A	EA	$\bar{y}$	$E\bar{y}A$	$E\bar{y}^2A$	$E\bar{I}$
330,000	1	.0005	165.0	.00025	.04125	.0000103125	$3.4375(10)^{-6}$
200,000	2	.0004	80.000	.0007	.0560	.0000392	$1.0666(10)^{-6}$
25,000	3	.0005	12.50	.00115	.014375	.00001653125	$2.60417(10)^{-6}$
			257.5		.111625	$6.604(10)^{-5}$	$4.7646(10)^{-6}$

$$\bar{Y} = \frac{\Sigma E\bar{y}A}{\Sigma EA} = .0004335;$$

$$R = \frac{.1580}{2} + \bar{y}; \text{or}$$

$$R = .07943''$$

$$\bar{E}\bar{I} = \Sigma E\bar{I} + \Sigma\bar{y}^2 AE - (\Sigma EA)\bar{y}^2$$

$$\bar{E}\bar{I} = 2.242(10)^{-5}\ \text{lb} - \text{in}^2$$

Equation 4 becomes as follows:

$$\theta = 30°$$

$$\alpha = \frac{I}{AR^2} = \frac{2.242(10)^{-5}}{257.5(.07943)^2} = 1.38(10)^{-5}; K_1 = 1$$

$$\beta = \frac{FEI}{GAR^2} \cong \frac{1.5(2.242)10^{-5}}{\left[10^5(1.4)(.07943)^2\right]} = 3.8(10)^{-8}; K_3 = 1.0$$

$$\delta = W\frac{(.07943)^3}{2.242(10)^{-5}}\left[\frac{1}{4\sin^2 30°}\left(\frac{\pi}{6} + \frac{\sin 60}{2}\right) - \frac{1}{\frac{\pi}{3}}\right] = .0376W - \text{in}$$

$$W = K\delta = 25.6\delta$$

Where K = constant of straw.

Amount that straw will be squeezed $\delta = .00160 = \frac{.1590 - .1558}{2}$

Pressure on shell of Module due to straw squeeze will be q lb/in^2

$$q = \frac{W}{\text{strawpitch}} = \frac{26.6(.00160)}{[.1558 + .0014(2)]} = .268\text{psi}$$

First determine bulge of 4 ply, $(\pm 30)_s$, without foam, and then with foam:

Roark, 5th Edition, pg. 386, case 1a,

$$\frac{a}{b} = \frac{31.5}{5.21} = 6.05$$

$$\Delta_b = \frac{\alpha q b^4}{E_{90} t^3} 5;$$

$$E = E_{90} = 3.51(10)^6$$

$$\alpha = .142$$

$$\Delta_b = \frac{.142(.268)(5.21)^4}{3.51(10)^6(.010)^3} = 7.97 - \text{in}$$

This does not provide adequate stiffness. Assume the following:

$\Delta_b = (7 \sin 60 + 1)\delta$ for 8 rows of straws.

So, when $\delta = .0016$, Δ_b should be less than (7 sin 60 + 1).0016 = .0113
To assure that this condition is met,

Replace t in Equation 3 with t*, where

$$\frac{(t^*)^3}{12} = \frac{h'^2(.010)}{4}$$

$$t^{*3} = .030h'^2$$

$$\Delta_b = .0113 = \frac{.142(.268)(5.21)^4}{3.51(10)^6(.030)h'^2}$$

$$h' = .1535 \text{ in}$$

0.154-in of foam reduces the flexibility by a factor of 7.99/.0113 or 707. (over 700 times as stiff as without the foam).

The use of 1.9 lb/ft^3 Rohacell WF Grade, .150 in thick foam increases the stiffness and weighs only as much as 1.07 plies of graphite epoxy. The transverse flexibility problem of the sides, top and bottom is solved by placing 0.015-in. foam in the sides of trough and 0.150-in of foam in the bottom and top of the module.

Instability due to one side of the trough or lid buckling before the other side does presents the final obstacle. We will first check the lid for this phenomenon.

Check the lid for twist-bend buckling. See appendix (see J.P. Den Hartog's Advanced Strength of Materials, page 283) for explanation of this buckling mode.

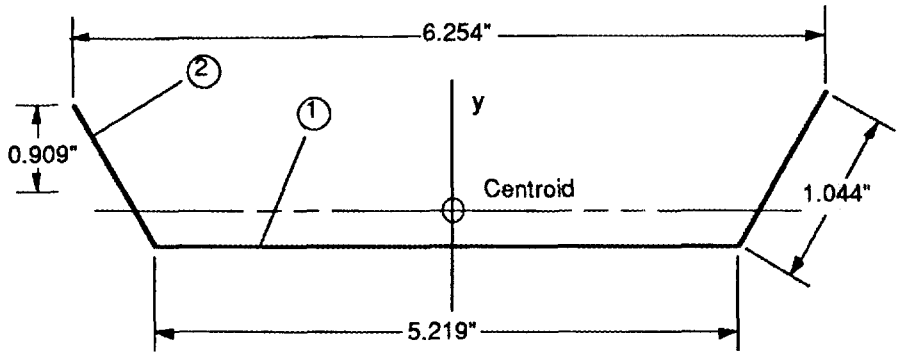

FIGURE 10 - Lid Top Dimensions

From the appendix, $M_{o_{critical}} \equiv M_o$, where

$$M_o = \frac{\pi\sqrt{EI_f \cdot C}}{l}$$

Item	A	$\bar{y}$	$A\bar{y}$	$A\bar{y}^2$	I
Trough	.0521	.005	$2.605(10)^{-4}$	$1.3025(10)^{-6}$	$4.3417(10)^{-7}$
Lid	.02088	.452	.0094378	.0042659	.0014218
			.0096983	.0042672	.0014222

analyzed for $[\pm 30]_s$.0025in/ply

$A = .07298$

$\bar{y} = .13289$ in

$I_f = .0014222 + .0042672 - .0096983\ (.13289)$
$= .00440\ in^4$

$C\theta = T$; or twist angle per in of length $= \frac{\theta}{L} = \frac{T}{C}$

See Roark, 5th Edition, page 300, case 1., C=KG

$$K = \frac{t^3}{3}(h + 2b) = \frac{(.010)^3}{3}[5.21 + 2(.904)] = 2.34(10)^{-6}$$

G of $[\pm 30]_s$ layup $= 6.39(10)^6$

$\therefore$ C =KG $= 14.95$ in^2 – lb

Equation 4 becomes:

$$M_o = \frac{\pi}{32''}\sqrt{20(10)^6(.00440)14.95}$$

$$M_o = 112.6 \text{ in} - \text{lb}$$

What differential stress and strain in the turned-up legs would produce this buckling moment:?

Determine I_{yy} from Figure above

$$I_{yy} = .010\frac{(5.21)^3}{12} + (1.044)(.010)2(2.866)^2 = .289 \text{ in}^4$$

$$\sigma = \frac{M_o C}{I} = \frac{(112.6)2.87}{.289} = 1{,}118 \text{ psi}$$

$$\text{Strain} = E = \frac{\sigma}{E} = \frac{1118}{20(10)^6} = .0000559\frac{\text{in}}{\text{in}}$$

Now, we should estimate what possible differential stress exists in the cured graphite epoxy.

Cured Graphite Epoxy Cools from 350°F to 70°F

$E_{epoxy} = 1(10)^6$ psi

$E_{graphite} = 60(10)^6$ psi

$$\Delta_e - \Delta_g = P_A\left[\frac{1}{A_e E_e} + \frac{1}{A_g E_g}\right]$$

$$P_A = \left(\frac{\Delta_E - \Delta_g}{\frac{1}{A_e E_e} + \frac{1}{A_g E_g}}\right) = \frac{(25 + 1.38)10^{-6}(-280)}{\left[\frac{1}{.40(10)^6} + \frac{1}{.60(60)10^6}\right]}$$

$$P_{.4} = -2922 \text{lb}$$

$$\text{stress in graphite} = \frac{P_{AO}}{.60} = \sigma_g$$

$$\sigma_g^{.4} = -4{,}870 \text{ psi compression}$$

Differential Stress in Flanges $= \sigma^{5}_{g} - \sigma^{4}_{g} = -2395$ psi

Also note that if one flange buckled before the other, twist-bend buckle would occur. The -2395 psi is more than twice the value required to buckle the lid in twist-bend.

Will foam will solve the twist-bend buckling problem?

To determine K(C=GK); use Roark, 5th Edition, a combination of case 1 (pg. 300) and case 16 (pg. 293):

Treat the case as two springs in parallel

$$(T = KG\theta)$$
$$T_1 + T_2 = T$$
$$T_T = GK_T = G(K_1 + K_2)$$
$$K_T = K_1 + K_2$$
$$K_1 = \frac{(.010)^3}{3} \cdot 2(.904) + \frac{(.005)^3(5.21)2}{3}$$
$$\text{or } K_1 = 6.027(10)^{-7} + 4.342(10)^{-7}$$
$$K_2 = \frac{2(.005)(5.125 - .005)^2(.16 - .005)^2}{(5.125 + .160 - .010)} = 1.19394(10)^{-3}$$

$$K_T = K_1 + K_2 = 1.1945(10)^{-3}$$
$$G = 6.39(10)^{-6}$$
$$C = GK_T = 7630 \text{ in}^2/\text{lb}$$

If I_f were the same,

$$M_o = \frac{\pi}{32}\sqrt{20(10)^6 .00440(7,630)}$$
$$= 2544$$

and the critical differential stress would be $\left(\sigma = \frac{MC}{I}\right)$ 25,300 psi

Thus, whereas the design without foam would buckle (twist bend) at a differential stress of only 1,118 psi, the design with .150-in of foam between the face sheets (of ±30 plies on each side), would require 25,300 psi differential stress. Thus, 0.150-in of foam necessary for minimizing bulging will also eliminate twist-bend buckling.

The results of this analysis indicate that 0.039-in foam in side walls and 0.150-in foam in the bottom and top of module (trough and lid) will prevent buckling and excessive bulging in the module.

5.0 Conclusion

Design and fabrication of support shells for the outer tracker of the SDC detector requires significant studies into the behavior of candidate materials and processes. The contradictory requirements of low mass, low deflection, and high thermal stability demand continued evaluations and development in the field of carbon-based composite materials. The results of studies of the cylindrical shell and modular shell are directly applicable to one another, and the two designs are progressing in a coordinated manner. This preliminary report presents the results of engineering studies conducted on the two shell configurations described above. The final results of this design task will be applicable to many additional fields requiring high precision, lightweight structures. The spin-off technologies from work on the Superconducting Super Collider project are only beginning to be realized.

Internal Distribution

1. G. T. Alley
2. C. M. Amonett
3. B. R. Appleton
4-6. H. G. Brashear
7. D. D. Cannon
8. F. C. Davis
9. T. E. Douglass
10. B. F. Elam
11. C. P. Frew
12-15. T. A. Gabriel
16-18. C. A. Hall
12. L. E. Johnson
13. R. M. Leitch
14. J. A. Mayhall
15. F. A. Modine
16-20. T. L. Ryan
21. A. W. Trivelpiece
22. R. M. Tuft
23-26. D. H. Vandergriff
27. Plant Records
28. R. W. Brockett (Consultant)
29. J. J. Dorning (Consultant)
30. J. E. Leiss (Consultant)
31. N. Moray (Consultant)
32. M. F. Wheeler (Consultant)
33. EPMD Reports Office
34-35. Laboratory Records Department
36. Laboratory Records, ORNL-RC
37. Document Reference Section
38. Central Research Library
39. ORNL Patent Section

External Distribution

40. Dr. John R. O'Fallon, Division of High Energy Physics, Department of Energy, ER-22/GTN, Washington, DC 20545
41. Office of Assistant Manager, Energy Research and Development, DOE-ORO, P. O. Box 2001, Oak Ridge, Tn 37831
42-52. Office of Scientific and Technical Information, Department of Energy, Oak Ridge, TN 37831
53. Muzzafer Atac, Fermi National Laboratory, P.O. Box 500, MS-233, WH14NE, Batavia, IL 60510
54. William L. Dunn, Quantum Research Services, Inc., 100 Capicola Dr., Suite 109, Durham, NC 27713-4411
55. W. T. Ford, University of Colorado, Physics 390, Boulder, CO 80309-0390
56. M. G. D. Gilchriese, Lawrence Berkeley Laboratory, One Cyclotron Road, MS-50A-2160, Berkeley, CA 94720
57. A. T. Goshaw, Duke University, Physics Dept., Durham, NC 27706
58. Gail Hanson, Indiana University, Physics Dept., Bloomington, N 47405
59. D. S. Koltick, Purdue University, Physics Dept., West Lafayette, IN 47907
60. Harold Ogren, Indiana University, Physics Dept., Bloomington, IN 47405
61. Seog Oh, Duke University, Physics Dept., Durham, NC 27706
62. Stephen Reucroft, Northeastern University, Physics Dept., Boston, MA 02115
63. Randy Ruchti, University of Notre Dame, Physics Dept., Notre Dame, IN 46556
64. George Trilling, Lawrence Berkeley Laboratory, One Cyclotron Road, MS 50A-2160, Berkeley, CA 94720